A combination of *Sophora flavescens* alkaloids and *Panax quinquefolium* saponins attenuates coxsackievirus B3-induced acute myocarditis in mice via NF-κB signaling

MENGHUI LIU[1,2], MEILING FAN[3], HUIBO XU[4], BO LIU[4], XIN WANG[4], FUCHUN WEN[4], FENGLAN JI[4] and TAO DING[4]

[1]Department of Pediatrics, Jilin Academy of Traditional Chinese Medicine, Changchun, Jilin 130012; [2]Department of Traditional Chinese Medicine, Changchun University of Traditional Chinese Medicine, Changchun, Jilin 130000; [3]Department of Cardiology, The First Affiliated Hospital of Changchun University of Chinese Medicine; [4]Pharmacodynamic and Toxicological Evaluation Center, Jilin Academy of Traditional Chinese Medicine, Changchun, Jilin 130012, P.R. China

Received January 25, 2023; Accepted April 14, 2023

DOI: 10.3892/etm.2023.11991

Abstract. Timely treatment of viral myocarditis (VMC), a form of cardiac inflammation caused by viral infections, can reduce the occurrence of dilated cardiomyopathy and sudden death. Our previous study demonstrated the anti-inflammatory and anti-fibrotic effects of KX, a combination of *Sophora flavescens* alkaloids and *Panax quinquefolium* saponins, on an autoimmune myocarditis model *in vivo*. The present study explored the effects of KX on coxsackievirus B3 (CVB3)-induced acute VMC in mice. Mice were randomly divided into four groups: Control, VMC, KX-high (275 mg/kg) and KX-low (138 mg/kg). Mice in the VMC, KX-high and KX-low groups received injections of CVB3 to establish the VMC model, and those in the KX-high and KX-low groups also received KX by gavage (10 ml/kg) 2 h after virus injection until euthanasia was performed on day 7 or 21. Mice in the control group received an equal KX volume of purified water. The levels of lactate dehydrogenase (LDH), creatine kinase-myocardial band (CK-MB), cardiac troponin I (cTn-I), IL-1β, IL-6, TNF-α and high-sensitive C-reactive protein (hs-CRP) in mouse serum was measured using ELISA. Myocardial tissue structure and degree of injury were observed using hematoxylin and eosin staining. Western blotting and reverse transcription-quantitative PCR were performed to detect the expression levels of NF-κB pathway-related mRNA and protein in myocardial tissue. The results showed that the inflammation and myocardial damage levels of the mice in the VMC group were higher at 7 days than those at 21 days. At both 7 and 21 days, KX decreased the serum CK-MB, LDH, cTn-I, IL-6, TNF-α and hs-CRP levels, and inhibited NF-κB pathway-related mRNA and protein expression in the myocardium of mice. These findings indicated that KX may reduce the inflammatory response and attenuate the pathological damage in the acute and subacute phases of CVB3-induced VMC through the NF-κB pathway.

Correspondence to: Dr Tao Ding, Pharmacodynamic and Toxicological Evaluation Center, Jilin Academy of Traditional Chinese Medicine, 155 Chuangju Street, Changchun, Jilin 130012, P.R. China
E-mail: dtdingtao@163.com

Abbreviations: KX, combination of Sophora flavescens alkaloids and Panax quinquefolium saponins; VMC, viral myocarditis; TCM, traditional Chinese medicine

Key words: Sophora flavescens alkaloids, *Panax quinquefolium* saponins, KX, VMC, acute myocarditis

Introduction

Viral myocarditis (VMC), a form of cardiac inflammation caused by viral infections, is a common and fatal disease, and one of the leading causes of dilated cardiomyopathy (DCM) and sudden death, threatening millions of lives worldwide, especially among children and young patients <40 years of age (1,2). Enteroviruses have long been recognized as the major etiological agents of VMC, accounting for ~25% of cases (3) and coxsackievirus B3 (CVB3) is considered to be a major causative virus (4). When a virus infects the heart, it causes direct damage to cardiomyocytes by binding the coxsackievirus and adenovirus receptor (CAR) and disrupting the cytoskeleton (5). This also leads to the activation of the immune system, the recruitment of immune cells, such as T lymphocytes, and the release of a large number of inflammatory factors, such as TNF-α, IL-1β and IL-6, which, together with the virus, aggravate the myocardial injury (6). Although the effectiveness of treatments for VMC, e.g., treatments targeting specific cytokines, such as IL-1β, has been demonstrated in clinical experiments and specific cases, 95% of patients receiving these treatments develop various degrees of adverse reactions (7,8). Inhibition of the inflammatory response to VMC is currently a valid and reliable therapeutic

approach (9). However, to the best of our knowledge, safe and effective drugs to inhibit these inflammatory responses are currently lacking.

Chinese herbal medicines are a major source of drugs that can play primary or adjuvant therapeutic roles in a variety of diseases (10). A previous pharmacological study demonstrated that matrine can ameliorate immunoinflammatory activity, and it has been shown to reduce the levels of TNF-α and IL-1β in a rheumatoid arthritis model through the NF-κB signaling pathway (11). *Panax quinquefolium* saponins have also been shown to present protective effects on cardiac injury, and improve cardiac fibrosis and cardiac remodeling in rats with heart failure (12,13). The main pharmacodynamic agents in *Sophora flavescens* are *Sophora flavescens* alkaloids, while the main pharmacodynamic agents in *Panax quinquefolium* are *Panax quinquefolium* saponins, which were combined in the present study to investigate the characteristics of this Chinese herbal medicine. KX, the drug obtained by combining *Sophora flavescens* alkaloids and *Panax quinquefolium* saponins, was previously shown to ameliorate cardiac inflammation and myocarditis-induced fibrosis in mice with autoimmune myocarditis (14). However, its role in the acute inflammatory phase of VMC remains unclear. Therefore, in the current study, we hypothesized that KX could ameliorate CVB3-induced VMC in mice and the underlying mechanism was explored. The present findings could provide an experimental basis for the clinical application of KX in patients with VMC.

Materials and methods

Animals and CVB3. A total of 120 male BALB/c mice aged 6-8 weeks (weight, 18-20 g) were purchased from Changchun Billion Laboratory Animal Technology Co., Ltd. [license no. SCXK (Liao)-2020-0002]. The mice were housed in an SPF environment at a temperature of 23±2˚C, 60±10% humidity and under a 12-h light/dark cycle. All animals had free access to food and water. The CVB3 strain was maintained at the Department of Pathogen Biology, Jilin University School of Basic Medical Sciences, Changchun, China. The virus was passaged and propagated in Vero cells; the cells were lysed three times through freeze-thawing, and their supernatants were harvested by centrifugation at 200 x g, 4˚C for 5 min and stored at -70˚C after aliquoting. Virus samples were serially diluted 10-fold. Then equal volumes of viral fluids were taken to infect Vero cells, respectively, and the number and proportion of cell wells exhibiting cytopathic effect were observed for 3-4 days after viral infection. Each dilution was assayed for its ability to induce cytopathic changes. The TCID50 of the virus could then be determined to be 10^6/ml by statistical analysis. The present study was approved by the Animal Ethics Committee of Jilin Academy of TCM (approval no. JLSZ KYDWLL2021-003; Changchun, China).

Composition, ratio and concentration selection of KX. *Sophora flavescens* alkaloids, consisting of matrine ($C_{15}H_{24}N_2O$) and oxymatrine ($C_{15}H_{24}N2O_2$) in a 1:1 ratio, were pure (HPLC purity, ≥98%). *Panax quinquefolium* saponins consisted of ginsenoside Rg1 ($C_{42}H_{72}O_{14}$), ginsenoside Re ($C_{48}H_{82}O_{18}$) and ginsenoside Rb1 ($C_{54}H_{92}O_{23}$), and their purity was determined to be ≥70% by high-performance liquid chromatography. These drugs were obtained from the new drug center of the Jilin Academy of TCM. The optimal total matrine to total saponin ratio from American ginseng was 1.1:1, as determined using an experimental model of autoimmune myocarditis and the optimal concentrations corresponding to high and low doses of KX were 275 and 138 mg/kg, respectively (14).

VMC induction and KX treatment. After 5 days of adaptive feeding, BALB/c mice were randomly divided into the following groups based on body weight (30 mice/group): i) Control; ii) VMC; iii) KX-high (275 mg/kg); and iv) KX-low (138 mg/kg). The specific grouping method is as follows: Mice were sequentially arranged in cages according to body weight, with the first round starting from the cage with the highest body weight and ending with the cage with the lowest body weight or vice versa. In the second round, the arrangement started from the second cage until the last cage, with the first cage containing two mice. In the third round, the arrangement started from the third cage until the last cage, with the first two cages supplemented with three mice. For the fourth round, the arrangement started from the fourth cage until the last cage, with the first three cages supplemented with four mice. This process was repeated starting from the first cage until all the mice were separated into cages with homogeneous body weights. All mice, except for those in the control group, received intraperitoneal injections of 0.1 ml CVB3 virus with a $TCID_{50}$ of 100, and KX or purified water 2 h later.

High- and low-dose KX solutions were prepared by dissolving 275 or 138 mg KX, respectively, in 10 ml distilled water. Mice in the KX-high and KX-low groups were intragastrically fed the experimental drug by gavage (10 ml/kg) daily from day 0 until sacrifice (day 7 or 21). Mice in the control and VMC groups received an equal volume of distilled water. All animals were anesthetized by intraperitoneal injection of sodium pentobarbital (50 mg/kg) and then euthanized by cervical dislocation. Mice (a total of 3 mice) that exhibited self-injuring behavior and nonhealing wounds were anesthetized by intraperitoneal injection of pentobarbital sodium (50 mg/kg), and then euthanasia was performed through cervical dislocation. Death was confirmed by the absence of breathing and heartbeat.

Histopathology. Mice were euthanized after 7 (40 mice; 10 mice/group) or 21 (40 mice; 10 mice/group) days and their body weight (BW) and heart weight (HW) were measured to calculate the cardiac index (HW/BW). The heart tissues were fixed in 15% formalin at 23±2˚C for >48 h, embedded in paraffin and sectioned into transverse sections (5 μm). Sections were stained with hematoxylin and eosin (H&E) at 23±2˚C for 5-20 min. The H&E-stained myocardial tissue sections were examined under a light microscope at x400 magnification and the macroscopic score was measured using the following five-point scale: 0, no inflammation; 1, limited discoloration; 2, numerous small lesions; 3, diffused discoloration not exceeding one-third of the heart surface; and 4, diffused discoloration exceeding one-third of the heart surface (15).

Cytokine ELISA. After anesthetizing the mice, blood was collected from the abdominal aorta. The whole blood was allowed to stand for 1 h at 23±2˚C, followed by centrifugation at 4˚C, 200 x g for 10 min, and then serum was obtained. Serum levels of creatine kinase-myocardial band (CK-MB), lactate dehydrogenase (LDH), cardiac troponin I (cTn-I), and the inflammatory markers IL-1β, IL-6, TNF-α and high-sensitive C-reactive protein (hs-CRP), were measured using the following mouse ELISA kits: (CK-MB; cat. no. YX-031115M; LDH; cat. no.YX-120408M; cTn-I; cat. no. YX-201409M; IL-1β; cat. no. YX-091203M; IL-6; cat. no. YX-091206M; TNF-α; cat no. YX-201407M; hs-CRP; cat. no. YX-081903M; all from SINOBESTBIO, Co., Ltd.). Standards (50 μl) were added into predefined wells of the microplates. Samples (10 μl serum) and sample diluent (40 μl) were added to the testing sample wells, while the blank wells were left empty. In the wells for standards and samples, horseradish peroxidase-labeled conjugates (100 μl) were added before sealing the plates for incubation at 37˚C for 60 min. After washing the plates five times, substrates A (50 μl) and B (50 μl) were added to each well. After incubation at 37˚C for 15 min, a stop solution (50 μl) was added to each well, and the absorbance of each well was measured at 450 nm within 15 min (cat. no. ELx800; BioTek Instruments, Inc.).

Reverse transcription-quantitative (RT-q)PCR. An appropriate amount of RNAiso plus (Takara Bio, Inc.) was added to the myocardial tissue and allowed to stand for 5 min at a temperature of 23±2˚C. Subsequently, RNAiso plus and one-fifth volume of chloroform were added and the solution was centrifuged at 12,000 x g for 15 min at 4˚C. The supernatant was then collected and pipetted into a new centrifuge tube. RNAiso plus and an equal volume of isopropanol were added and allowed to stand for 10 min at room temperature; thereafter, the solution was centrifuged at 12,000 x g for 10 min at 4˚C. The supernatant was removed and an equal volume of 75% ethanol to RNAiso plus was added. The supernatant was carefully discarded after centrifugation at 7,500 x g for 5 min at 4˚C and the samples were stored after drying. The RNA was then reverse-transcribed into cDNA with the RT Kit (GoScript™ Reverse Transcription; cat. no. A5001; Promega Corporation), which was amplified via qPCR (SystemGoTaq® qPCR Master Mix; cat. no. A6001; Promega, Inc.). qPCR was performed using the following thermocycling conditions: Initial denaturation at 95˚C for 10 min, followed by 40 cycles of 95˚C for 15 sec and 60˚C for 60 sec. The $2^{-\Delta\Delta Cq}$ method was used to calculate the relative content of mRNA using GAPDH as the internal reference gene (16). The following primer sequences were used for qPCR: IκBα forward, 5'-ATCCTG ACCTGGTTTCGCTC-3' and reverse, 5'-TGGTAGGGGGAG TAGCCTTG-3'; NF-κB P65 forward, 5'-CCTCTGGCGAAT GGCTTTAC-3' and reverse, 5'-TGCTTCGGCTGTTCGATG AT-3'; GAPDH forward 5'-TGGTGAAGGTCGGTGTGA AC-3', and reverse 5'-ACTGTGCCGTTGAATTTGCC-3'.

Western blotting. An appropriate amount of mouse myocardial tissue was weighed and added to the RIPA lysis buffer (cat. no. CW2333S; CoWin Biosciences) containing protease and phosphatase inhibitors in a 1:9 ratio. This was ground using a high-speed tissue grinder for 2 min, left to stand on ice for 20 min, centrifuged at 14,000 x g at 4˚C for 10 min and the supernatant stored in a -80˚C freezer. The total protein concentration in the sample was measured according to the instructions of the BCA protein concentration assay kit (cat.no. P0012S, Beyotime Biotechnology, shanghai, china). Samples containing 50 μg total protein were added to each lane to perform electrophoresis. Proteins were separated by SDS-PAGE on a 10% gel and transferred onto nitrocellulose membranes. After blocking in 5% non-fat milk diluted in TBS-0.1% Tween-20 (CoWin Biosciences) in the dark at 4˚C overnight, the membranes were incubated with primary antibodies (Santa Cruz Biotechnology, Inc.) against TGF-β-activated kinase 1 (TAK1)-binding protein 1 (TAB1; 1:100; cat. no. sc-166138), NF-κB (1:200; cat. no. sc-8008), phosphorylated (p)-NF-κB (1:200; cat. no. sc-136548), IκB (1:100; cat. no. sc-74451), p-IκB (1:200; cat. no. sc-390622) or GAPDH (1:100; cat. no. sc-365062) for 2 h at 37˚C. Subsequently, the membranes were washed with TBS-0.1% Tween 20 and incubated with a secondary HRP-conjugated antibody m-IgGκ (1:1,000; cat. no. sc-516102) or m-IgG-Fc (1:1,000; cat. no. sc-525409; both from Santa Cruz Biotechnology, Inc.) for 1.5 h at 37˚C. The membranes were then washed again and visualized using an enhanced chemiluminescence detection kit (cat. no. CW0049M, CoWin Biosciences). The levels of target proteins were normalized to those of GAPDH using a gel imaging system (ChemiDoc-It 510 Imager; Ultra-Violet Products, Ltd.). Protein bands were analyzed using ImageJ software (version 1.5.1; National Institutes of Health).

Statistical analysis. GraphPad Prism software (version 9.0 for Mac; GraphPad Software; Dotmatics) was used to perform the statistical analysis. Survival analysis was performed using Kaplan-Meier analysis followed by the Log-rank test. When two variables were being assessed, a two-way ANOVA with Bonferroni post hoc test was performed, while other comparisons were performed using one-way ANOVA followed by Tukey's post hoc test or Kruskal-Wallis test followed by Dunn's post hoc test. The macroscopic scores were presented as median ± interquartile range, while all other values were presented as mean ± standard deviation. $P<0.05$ was considered to indicate a statistically significant difference.

Results

Effects of KX on mouse survival and cardiac index. All mice developed symptoms such as apathy, decreased activity, clumping, eating less and dull fur starting 2-3 days after virus injection and some of the mice developed piloerection, which was progressively aggravated. The survival of mice in the VMC group was significantly lower compared with that in the control group ($P<0.05$; Fig. 1A); however, high-dose KX treatment significantly improved the survival of mice in comparison with that in the VMC group ($P<0.05$), while low-dose KX treatment had no significant effect ($P>0.05$) (Fig. 1A). After 7 days, mice in the VMC group weighed significantly less than those in the control group ($P<0.01$; Fig. 1B). In comparison with mice in the VMC group, mice that received KX showed a significant increase in weight ($P<0.01$; Fig. 1B). In comparison

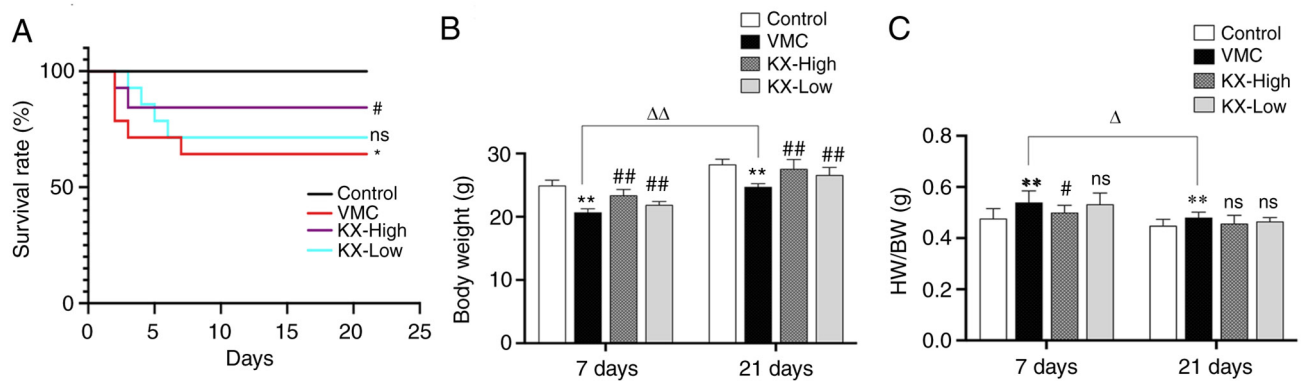

Figure 1. Effects of KX on survival and the cardiac index in mice with VMC. (A) Survival rate of mice. (B) BW changes in mice after 7 and 21 days of KX treatment (n=10/group). (C) Changes in HW/BW at 7 and 21 days (n=10/group). Two-way ANOVA and Bonferroni post hoc test: *P<0.05 and **P<0.01 vs. control; ^{ns}P>0.05, $^{\#}$P<0.05 and $^{\#\#}$P<0.01 vs. VMC; $^{\Delta}$P<0.05 and $^{\Delta\Delta}$P<0.01 vs. VMC (7 days). KX, combination of *Sophora flavescens* alkaloids and *Panax quinquefolium saponins*; VMC, viral myocarditis; ns, not significant; BW, body weight; HW, heart weight.

with that in the VMC group, the high-dose KX group showed a significant reduction in the cardiac index (P<0.05; Fig. 1C); however, the low-dose KX group showed no significant changes in cardiac index (P>0.05; Fig. 1C).

After 21 days, mice in the VMC group weighed significantly less compared with those in the control group (P<0.01), while mice in the KX intervention groups showed a significant increase in weight (P<0.01) (Fig. 1B). HW/BW in the VMC group was significantly higher than that in the control group (P<0.01; Fig. 1C); however, in comparison with the VMC group, the KX intervention groups did not show significant changes in HW/BW (P>0.05) (Fig. 1C). In comparison with the VMC mice euthanized at 7 days, the VMC mice euthanized at 21 days showed greater weight gain (P<0.05; Fig. 1A and B) and a lower HW/BW (P<0.05; Fig. 1C).

Effects of KX on myocardial injury in mice. After 7 days, the serum levels of LDH, CK-MB and cTn-I were significantly increased in the VMC group compared with those in the control group (P<0.01; Fig. 2A-C). In comparison with the VMC group, the KX intervention groups showed significant reductions in the serum levels of the aforementioned indicators (P<0.01; Fig. 2A-C). H&E staining of cardiac tissue showed significant inflammatory cell infiltration and damage to cardiac tissue in the VMC group on day 7 (P<0.01), while the inflammatory damage was significantly reduced after KX-high-dose intervention (P<0.05; Fig. 2G).

After 21 days, the serum CK-MB and LDH levels in the VMC mice were significantly higher than those in the controls (P<0.01 or P<0.05; Fig. 2D and E). In comparison with the VMC group, the KX-high-dose group showed a significantly lower LDH level (P<0.05), while the KX-low-dose group showed no significant change (P>0.05; Fig. 2D). Besides, KX had no significant effect on CK-MB (P>0.05; Fig. 2E). cTn-I expression did not differ significantly between the VMC and control groups (P>0.05; Fig. 2F). H&E staining of myocardial tissue showed inflammatory cell infiltration in the VMC group at 21 days, but myocardial tissue damage and inflammation were significantly reduced after KX-high-dose intervention in comparison with the VMC group (P<0.05; Fig. 2H).

Effects of KX on inflammatory factors in mouse serum. After 7 days, the levels of IL-6, IL-1β, TNF-α and hs-CRP were significantly increased in the VMC group compared with those in the control group (P<0.01; Fig. 3A-D). However, in comparison with the VMC group, the KX intervention groups showed a significant decrease in the levels of IL-6, IL-1β, TNF-α and hs-CRP (P<0.01; Fig. 3A-D) with a dose-effect relationship.

After 21 days, the levels of IL-6, TNF-α and hs-CRP were significantly increased in the VMC group compared with those in the control group (P<0.01 or P<0.05; Fig. 3E, F and H), whereas IL-1β levels did not change significantly (P>0.05; Fig. 3G). In comparison with the VMC group, the high-dose KX group showed significantly lower levels of IL-6, TNF-α and hs-CRP (P<0.01 or P<0.05; Fig. 3E, F and H), while the low-dose KX group showed significantly decreased TNF-α levels (P<0.01) but no significant changes in the IL-6, hs-CRP and IL-1β levels (P>0.05) (Fig. 3E-H).

Effects of KX on the NF-κB pathway in mouse myocardium. After 7 days, the protein expression levels of TAB1, p-IκB/IκB and p-NF-κB/NF-κB in the myocardium of mice in the VMC group were significantly increased compared with those in the control group (P<0.01; Fig. 4A-D). KX intervention resulted in a significant decrease in the myocardial levels of all of the aforementioned indicators (P<0.01 or P<0.05; Fig. 4A-D) and the results showed a dose-dependent pattern. The mRNA expression levels of NF-κB and IκB in the mouse myocardium were significantly increased in the VMC group compared with those in the control group (P<0.01) and their expression levels were significantly decreased after KX intervention (P<0.01 or P<0.05) (Fig. 4E and F), with the reduction showing a dose-effect relationship.

After 21 days, the myocardial protein expression levels of TAB1, p-IκB/IκB and p-NF-κB/NF-κB in the VMC group were significantly increased compared with those in the control group (P<0.01; Fig. 5A-D). Nonetheless, the myocardial levels of all of the aforementioned indicators were significantly decreased after high-dose KX treatment (P<0.01 or P<0.05; Fig. 5A-D); by contrast, low-dose KX treatment decreased the levels of p-NF-κB/NF-κB (P<0.05; Fig. 5C), but had no

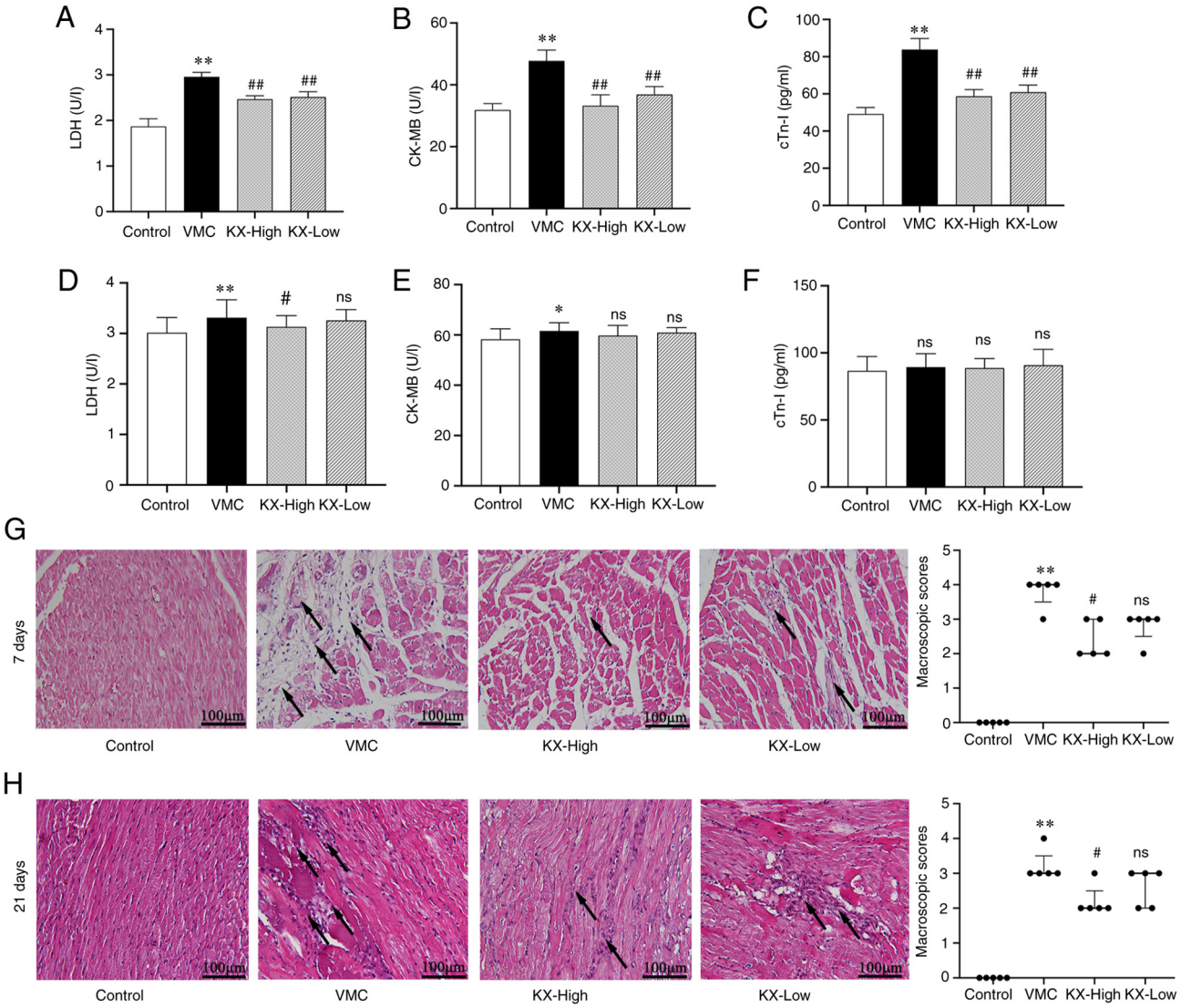

Figure 2. Effects of KX on myocardial injury in mice with VMC. Changes in the serum levels of (A) LDH, (B) CK-MB and (C) CTn-I after 7 days of KX treatment (Dunn's post hoc test). Changes in the serum levels of (D) LDH, (E) CK-MB, and (F) cTn-I after 21 days of KX treatment (One-way ANOVA and Tukey's post hoc test). (G and H) Hematoxylin and eosin staining of the myocardium (One-way ANOVA and Dunn's post-hoc test; n=5/group). Scale bars, 100 μm. Arrows indicate inflammatory cell infiltration (mainly lymphocytes) and myocardial injury. Quantified data plots are shown (macroscopic scores were compared among the groups). *P<0.05 and **P<0.01 vs. control; ^{ns}P>0.05, $^{\#}$P<0.05 and $^{\#\#}$P<0.01 vs. VMC. KX, combination of *Sophora flavescens* alkaloids and *Panax quinquefolium* saponins; LDH, lactate dehydrogenase; CK-MB, creatine kinase-myocardial band; cTn-I, cardiac troponin I; VMC, viral myocarditis; ns, not significant.

significant effect on TAB1 and p-IκB/IκB expression (P>0.05; Fig. 5B and D). Similarly, the mRNA expression levels of NF-κB and IκB in the myocardium of the mice in the VMC group were significantly increased compared with those in the control group (P<0.01), whereas they were significantly reduced (P<0.01 or P<0.05) after high-dose KX intervention but were not affected by low-dose KX intervention (P>0.05) (Fig. 5E and F).

Discussion

VMC is characterized by an acute onset, and complex and no specificity symptoms such as asthenia and shortness of breath (17). According to the TCM theory of treatment, the combination of *Sophora flavescens* alkaloids and *Panax quinquefolium* saponins shows good curative effects in the treatment of VMC, which displays the characteristic of TCM, including synergistic effects and advantages of drug combinations (14). KX has recently been shown to be effective in alleviating chronic inflammation and the degree of myocardial fibrosis in myocarditis (14,18). To clarify whether the impact of KX treatment on VMC extends throughout the entire pathological development process, the present study established a CVB3-induced acute VMC model and explored the effect of KX on acute inflammation in VMC. The results showed that KX attenuated VMC-related injury and inflammation levels possibly through the NF-κB pathway.

The CVB3-induced murine VMC model is commonly used to study the reaction phase of acute inflammation in VMC (19). Viral infection of the heart results in a series of pathological responses, which are mainly divided into three phases: An acute inflammatory phase (1-7 days), a subacute inflammatory

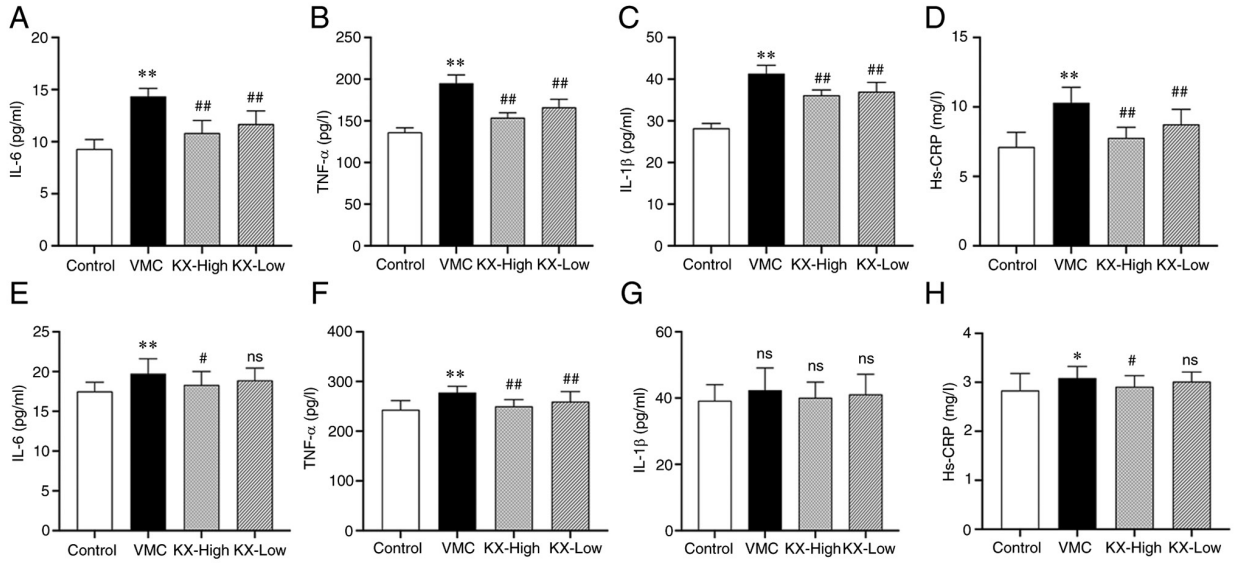

Figure 3. Effects of KX on the inflammatory factors in the serum of mice with VMC. (A) IL-6, (B) TNF-α, (C) IL-1β and (D) hs-CRP levels in the serum of mice with VMC after 7 days of KX treatment. (E) IL-6, (F) TNF-α, (G) IL-1β and (H) hs-CRP levels in the serum of mice with VMC after 21 days of KX treatment (n=10/group). One-way ANOVA and Dunn's post hoc test comparisons: *P<0.05 and **P<0.01 vs. control; ^{ns}P>0.05, $^{\#}$P<0.05 and $^{\#\#}$P<0.01 vs. VMC. KX, combination of *Sophora flavescens* alkaloids and P*anax quinquefolium* saponins; VMC, viral myocarditis; ns, not significant; hs-CRP, high-sensitive C-reactive protein.

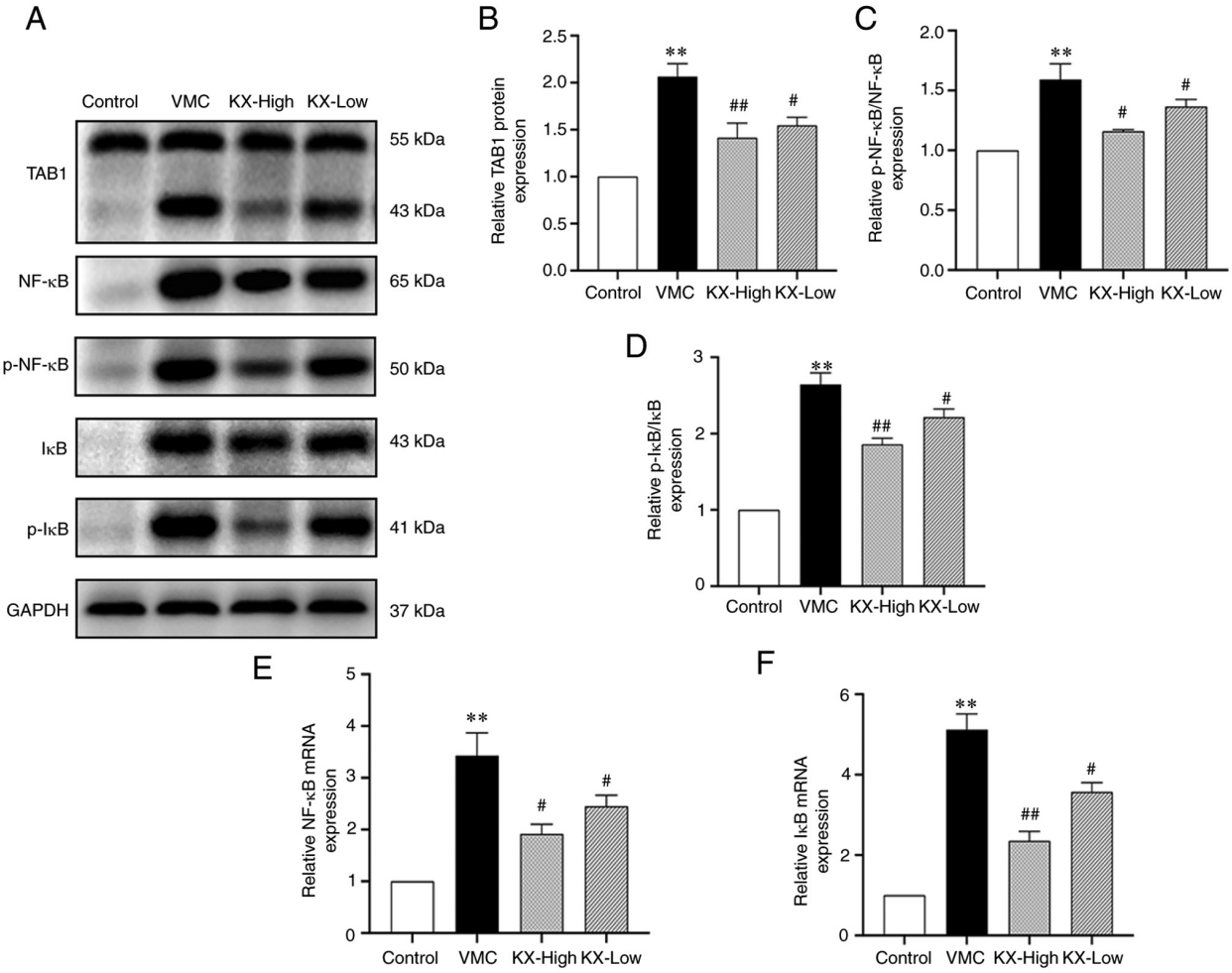

Figure 4. Effects of KX on the NF-κB pathway in mouse myocardium. (A) TAB1, NF-κB, p-NF-κB, IκB and p-IκB expression levels in the murine myocardium after 7 days of KX treatment. Western blot semi-quantification analysis (n=4/group) of (B) TAB1, (C) p-NF-κB/NF-κB and (D) p-IκB/IκB protein expression. Expression of (E) NF-κB and (F) IκB mRNA in mouse myocardium after 7 days of KX treatment. One-way ANOVA and Dunn's post hoc test comparisons: **P<0.01 vs. control; $^{\#}$P<0.05 and $^{\#\#}$P<0.01 vs. VMC. TAB1, TGF-β-activated kinase 1-binding protein 1; VMC, viral myocarditis; KX, combination of *Sophora flavescens* alkaloids and *Panax quinquefolium* saponins; p-, phosphorylated.

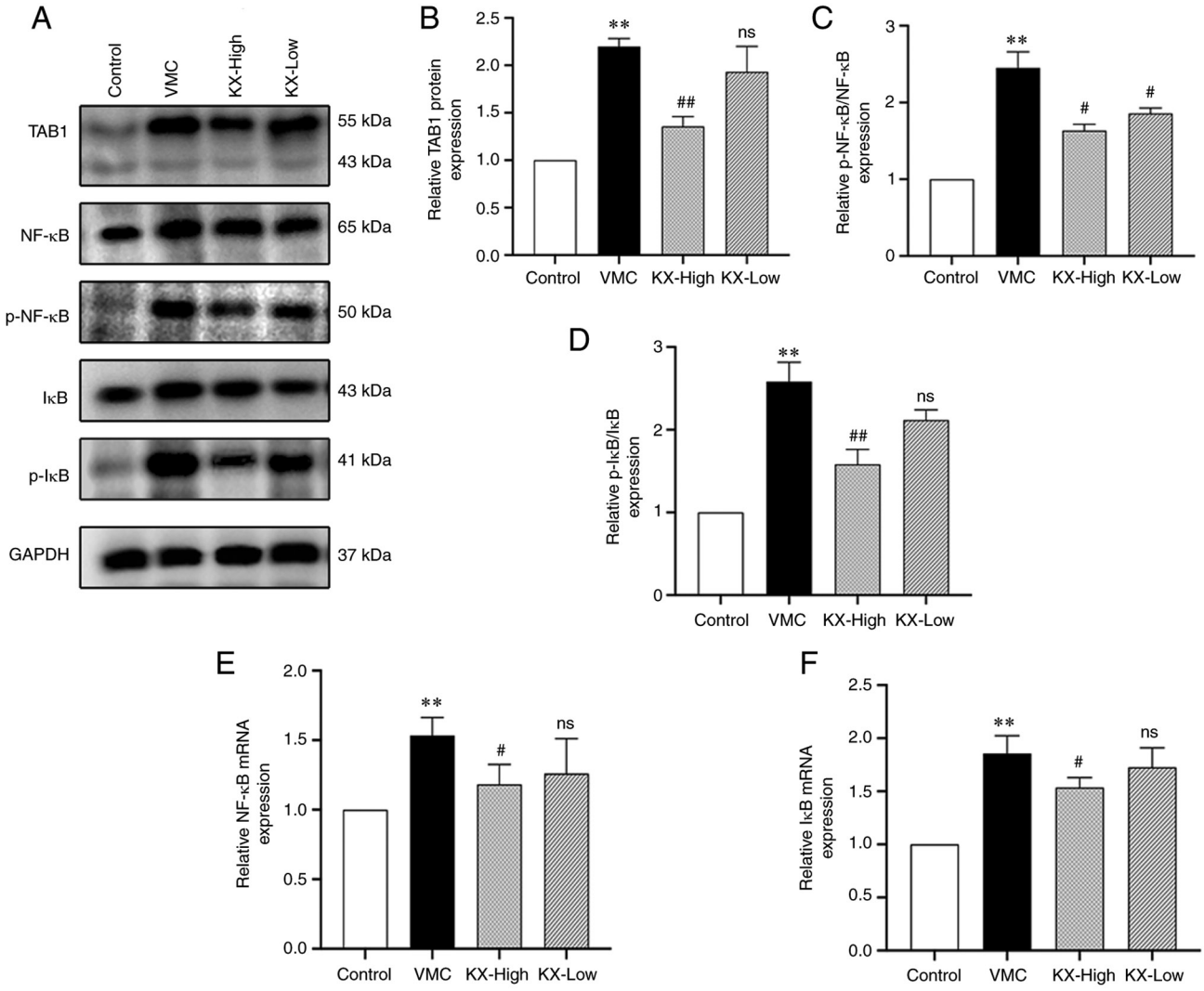

Figure 5. Effects of KX on the NF-κB pathway in mouse myocardium. (A) TAB1, NF-κB, p-NF-κB, IκB and p-IκB protein expression levels in the murine myocardium after 21 days of KX treatment. Western blot semi-quantification analysis (n=4/group) of (B) TAB1, (C) p-NF-κB/NF-κB and (D) p-IκB/-IκB protein expression. Expression of (E) NF-κB and (F) IκB mRNA in the mouse myocardium after 21 days of KX treatment. One-way ANOVA and Dunn's post hoc test comparisons, **P<0.01 vs. control; ^{ns}P>0.05, $^{\#}$P<0.05 and $^{\#\#}$P<0.01vs. VMC. TAB1, TGF-β-activated kinase 1-binding protein 1; VMC, viral myocarditis; KX, combination of *Sophora flavescens* alkaloids and *Panax quinquefolium* saponins; p-, phosphorylated.

phase (7-21 days) and a chronic inflammatory phase (after ~21 days) (6,20). In the acute phase, CVB3 enters the myocardium with the aid of a CAR, which damages cardiomyocytes (21), and the host immune response is subsequently induced. It has been shown that the inflammatory response leads to the transmigration of macrophages, T lymphocytes and natural killer cells to the site of injury, and the production of high levels of proinflammatory factors, such as IL-6, IL-1β and TNF-α. Together with the virus, these proinflammatory factors further aggravate cardiac damage through the cleavage of dystrophin by enteroviral protease 2A (22). In the subacute phase, viral replication and myocardial inflammation are reduced under the regulation of the autoimmune system (23); however, persistent myocardial inflammation can lead to fibrosis and DCM (24,25). Therefore, inhibition of myocardial inflammatory responses in the acute and subacute phases is an important step in treating VMC. Inhibition of TNF-α, IL-6 and IL-1β secretion was recently shown to effectively attenuate myocardial inflammatory injury (26,27). Simultaneous neutralization of TNF-α or IL-1β by antibodies or soluble receptors could attenuate the inflammatory response in VMC (28,29). In the present study, all mice developed symptoms such as apathy, decreased activity, clumping, eating less and dull fur starting 2-3 days after virus injection and some of the mice developed piloerection, which was progressively aggravated. Nonetheless, all the symptoms improved significantly after KX treatment. Nearly all mice injected with the virus were affected by VMC. In addition, significant myocardial inflammation and damage appeared in the mice after 7 days and some of the inflammation and damage persisted until day 21 under the regulation of the autoimmune system, which is consistent with the findings of a recent study (30). After the treatment of mice in the VMC group with KX, the levels of TNF-α, IL-6, IL-1β and hs-CRP were decreased in a dose-dependent manner, which played an important role in attenuating myocardial injury.

The NF-κB pathway is a classical proinflammatory signaling pathway mainly based on the role of NF-κB in the expression of proinflammatory genes, including cytokines, chemokines and adhesion molecules (31). TAB1 is a protein activator of TAK1,

and the TAB1-TAK1 complex phosphorylates the IκB kinase complex, which then induces phosphorylation of Ser32 and Ser36 residues in IκB, leading to its degradation and the activation of NF-κB (32). IL-1β, TNF-α and IL-6 overexpression can activate NF-κB via the TAB1 pathway. As a transcription factor, the activated NF-κB translocates into the nucleus to promote inflammation or the expression of inflammatory cytokines (33), leading to a cascade amplification of inflammatory cytokines and further resulting in persistent necrosis of cardiomyocytes and infiltration of inflammatory cells. Therefore, the TAB1/NF-κB pathway plays a key role in regulating inflammation, and inhibition of TAB1 and activation of the NF-κB pathway are effective in attenuating inflammation in the myocardium (26,34-36). Several studies have shown that *Momordica charantia* can act through NF-κB signaling pathways to reduce the level of inflammation in rheumatoid arthritis or models (11,37). In the present study, KX intervention in VMC mice attenuated myocardial injury in a dose-dependent manner and decreased TAB1 expression as well as the NF-κB pathway-related mRNA and protein expression levels. Thus, the KX formula may act through the TAB1/NF-κB pathway to reduce the level of inflammation and thereby ameliorate myocardial injury.

The present findings indicated that KX could effectively attenuate the inflammatory response in the acute and subacute phases of VMC, thereby providing an experimental basis for the clinical application of KX and indicating its effectiveness in reducing the clinical symptoms of acute VMC. However, the present study presented some limitations. The current study lacked a positive control group. Although *Astragalus membranaceus* and ribavirin were selected as positive drugs for VMC (38,39), their effectiveness remains unclear, especially in the subacute stage of VMC. Moreover, findings based on echocardiography, which is critical for cardiac function assessment in mice, were not obtained. Furthermore, it was difficult to identify which component of KX was involved in inflammation at different stages of VMC. In future work, the five components in KX could be isolated to perform experiments in VMC mice at different stages to identify which of them exert anti-inflammatory effects. Moreover, more accurate experiments could be performed to determine inflammation and protein expression localization of myocardium and determine if there is any difference between the right and left ventricles in the H&E staining or immunohistochemical methods.

Nevertheless, the present study suggested that KX could act through the TAB1/NF-κB pathway to decrease the inflammatory response in the acute and subacute phases of CVB3-induced VMC and thereby alleviate pathological damage. These findings partly embody the mechanism of action of KX in treating VMC with multiple components and targets and represent the synergistic effects and advantages of drug combinations of TCM formulas in treating VMC.

Acknowledgements

Not applicable.

Funding

The present study was supported by the Jilin Science and Technology Development Plan Project (grant no. 20200403128SF).

Availability of data and materials

The datasets used and/or analyzed during the current study are available from the corresponding author on reasonable request.

Authors' contributions

TD made substantial contributions to the conception and design of the study. ML and TD were responsible for the experimental procedures, data acquisition, analysis and interpretation, and confirmed the authenticity of all the raw data. ML performed the drafting of the article and critically revised it for important intellectual content.

were responsible for participating in the experiments and confirm the authenticity of all the raw data. All authors read and approved the final manuscript. All authors agree to be accountable for all aspects of the work in ensuring that questions related to the accuracy or integrity of the work are appropriately investigated and resolved.

Ethics approval and consent to participate

All experiments and animal care procedures were approved by the Animal Ethics Committee of Jilin Academy of Traditional Chinese Medicine (approval no. JLSZKYDWLL2021-003).

Patient consent for publication

Not applicable.

Competing interests

The authors declare that they have no competing interests.

References

1. Putschoegl A and Auerbach S: Diagnosis, evaluation, and treatment of myocarditis in children. Pediatr Clin North Am 67: 855-874, 2020.
2. Doolan A, Langlois N and Semsarian C: Causes of sudden cardiac death in young Australians. Med J Aust 180: 110-112, 2004.
3. Fairley CK, Ryan M, Wall PG and Weinberg J: The organisms reported to cause infective myocarditis and pericarditis in England and Wales. J Infect 32: 223-225, 1996.
4. Woodruff JF: Viral myocarditis. A review. Am J Pathol 101: 425-484, 1980.
5. He Y, Chipman PR, Howitt J, Bator CM, Whitt MA, Baker TS, Kuhn RJ, Anderson CW, Freimuth P and Rossmann MG: Interaction of coxsackievirus B3 with the full length coxsackievirus-adenovirus receptor. Nat Struct Biol 8: 874-878, 2001.
6. Pollack A, Kontorovich AR, Fuster V and Dec GW: Viral myocarditis-diagnosis, treatment options, and current controversies. Nat Rev Cardiol 12: 670-680, 2015.
7. Brucato A, Imazio M, Gattorno M, Lazaros G, Maestroni S, Carraro M, Finetti M, Cumetti D, Carobbio A, Ruperto N, *et al*: Effect of anakinra on recurrent pericarditis among patients with colchicine resistance and corticosteroid dependence: The AIRTRIP randomized clinical trial. JAMA 316: 1906-1912, 2016.
8. Scott IC, Hajela V, Hawkins PN and Lachmann HJ: A case series and systematic literature review of anakinra and immunosuppression in idiopathic recurrent pericarditis. J Cardiol Cases 4: e93-e97, 2011.

9. Tschöpe C, Ammirati E, Bozkurt B, Caforio ALP, Cooper LT, Felix SB, Hare JM, Heidecker B, Heymans S, Hübner N, *et al*: Myocarditis and inflammatory cardiomyopathy: Current evidence and future directions. Nat Rev Cardiol 18: 169-193, 2021.
10. Li FS and Weng JK: Demystifying traditional herbal medicine with modern approach. Nat Plants 3: 17109, 2017.
11. Niu Y, Dong Q and Li R: Matrine regulates Th1/Th2 cytokine responses in rheumatoid arthritis by attenuating the NF-κB signaling. Cell Biol Int 41: 611-621, 2017.
12. Zheng X, Wang S, Zou X, Jing Y, Yang R, Li S and Wang F: Ginsenoside Rb1 improves cardiac function and remodeling in heart failure. Exp Anim 66: 217-228, 2017.
13. Wang QW, Yu XF, Xu HL, Zhao XZ and Sui DY: Ginsenoside re improves isoproterenol-induced myocardial fibrosis and heart failure in rats. Evid Based Complement Alternat Med 2019: 3714508, 2019.
14. Liu M, Lin Y, Xu H, Li L and Ding T: Combination of *Sophora flavescens* alkaloids and *Panax quinquefolium* saponins modulates different stages of experimental autoimmune myocarditis via the NF-κB and TGF-β1 pathways. Exp Ther Med 24: 570, 2022.
15. Aretz HT: Myocarditis: The dallas criteria. Hum Pathol 18: 619-624, 1987.
16. Livak KJ and Schmittgen TD: Analysis of relative gene expression data using real-time quantitative PCR and the 2(-Delta Delta C(T)) method. Methods 25: 402-408, 2001.
17. Sinagra G, Anzini M, Pereira NL, Bussani R, Finocchiaro G, Bartunek J and Merlo M: Myocarditis in clinical practice. Mayo Clin Proc 91: 1256-1266, 2016.
18. Liu M, Lin Y, Xu H, Wang X, Liu B, Fan M, Ding T and Li L: Mechanism of the combination of KuShen and XiYangShen on myocarditis based on network pharmacology and animal experiments. Pharmacol Res-Mod Chin Med 4: 100141, 2022.
19. Błyszczuk P: Myocarditis in humans and in experimental animal models. Front Cardiovasc Med 6: 64, 2019.
20. Lasrado N and Reddy J: An overview of the immune mechanisms of viral myocarditis. Rev Med Virol 30: 1-14, 2020.
21. Kandolf R, Ameis D, Kirschner P, Canu A and Hofschneider PH: In situ detection of enteroviral genomes in myocardial cells by nucleic acid hybridization: An approach to the diagnosis of viral heart disease. Proc Natl Acad Sci USA 84: 6272-6276, 1987.
22. Badorff C, Lee GH, Lamphear BJ, Martone ME, Campbell KP, Rhoads RE and Knowlton KU: Enteroviral protease 2A cleaves dystrophin: Evidence of cytoskeletal disruption in an acquired cardiomyopathy. Nat Med 5: 320-326, 1999.
23. Huber SA, Sartini D and Exley M: Vgamma4(+) T cells promote autoimmune CD8(+) cytolytic T-lymphocyte activation in coxsackievirus B3-induced myocarditis in mice: Role for CD4(+) Th1 cells. J Virol 76: 10785-10790, 2002.
24. Izumi T, Takehana H, Matsuda C, Yokoyama H, Kohno K, Suzuki K and Inomata T: Experimental autoimmune myocarditis and its pathomechanism. Herz 25: 274-278, 2000.
25. Esfandiarei M and McManus BM: Molecular biology and pathogenesis of viral myocarditis. Annu Rev Pathol 3: 127-155, 2008.
26. Liu T, Zhang M, Niu H, Liu J, Ruilian M, Wang Y, Xiao Y, Xiao Z, Sun J, Dong Y and Liu X: Astragalus polysaccharide from Astragalus Melittin ameliorates inflammation via suppressing the activation of TLR-4/NF-κB p65 signal pathway and protects mice from CVB3-induced virus myocarditis. Int J Biol Macromol 126: 179-186, 2019.
27. Gu X, Li Y, Chen K, Wang X, Wang Z, Lian H, Lin Y, Rong X, Chu M, Lin J and Guo X: Exosomes derived from umbilical cord mesenchymal stem cells alleviate viral myocarditis through activating AMPK/mTOR-mediated autophagy flux pathway. J Cell Mol Med 24: 7515-7530, 2020.
28. Kubota T, Bounoutas GS, Miyagishima M, Kadokami T, Sanders VJ, Bruton C, Robbins PD, McTiernan CF and Feldman AM: Soluble tumor necrosis factor receptor abrogates myocardial inflammation but not hypertrophy in cytokine-induced cardiomyopathy. Circulation 101: 2518-2525, 2000.
29. Kraft L, Erdenesukh T, Sauter M, Tschöpe C and Klingel K: Blocking the IL-1β signalling pathway prevents chronic viral myocarditis and cardiac remodeling. Basic Res Cardiol 114: 11, 2019.
30. Yue-Chun L, Gu XH, Li-Sha G, Zhou DP, Xing C, Guo XL, Pan LL, Song SY, Yu LL, Chen GY, *et al*: Vagus nerve plays a pivotal role in CD4+ T cell differentiation during CVB3-induced murine acute myocarditis. Virulence 12: 360-376, 2021.
31. Sen R and Baltimore D: Multiple nuclear factors interact with the immunoglobulin enhancer sequences. Cell 46: 705-716, 1986.
32. Shim JH, Xiao C, Paschal AE, Bailey ST, Rao P, Hayden MS, Lee KY, Bussey C, Steckel M, Tanaka N, *et al*: TAK1, but not TAB1 or TAB2, plays an essential role in multiple signaling pathways in vivo. Genes Dev 19: 2668-2681, 2005.
33. Cheng Z, Taylor B, Ourthiague DR and Hoffmann A: Distinct single-cell signaling characteristics are conferred by the MyD88 and TRIF pathways during TLR4 activation. Sci Signal 8: ra69, 2015.
34. Xue YL, Zhang SX, Zheng CF, Li YF, Zhang LH, Hao YF, Wang S and Li XW: Silencing of STAT4 protects against autoimmune myocarditis by regulating Th1/Th2 immune response via inactivation of the NF-κB pathway in rats. Inflammation 42: 1179-1189, 2019.
35. Pan A, Tan Y, Wang Z and Xu G: STAT4 silencing underlies a novel inhibitory role of microRNA-141-3p in inflammation response of mice with experimental autoimmune myocarditis. Am J Physiol Heart Circ Physiol 317: H531-H540, 2019.
36. Zhu Z, Xueying L, Chunlin L, Wen X, Rongrong Z, Jing H, Meilan J, Yuwei X and Zili W: Effect of berberine on LPS-induced expression of NF-κB/MAPK signalling pathway and related inflammatory cytokines in porcine intestinal epithelial cells. Innate Immun 26: 627-634, 2020.
37. Hu J, Luo J, Zhang M, Wu J, Zhang Y, Kong H, Qu H, Cheng G and Zhao Y: Protective effects of radix sophorae flavescentis carbonisata-based carbon dots against ethanol-induced acute gastric ulcer in rats: Anti-inflammatory and antioxidant activities. Int J Nanomedicine 16: 2461-2475, 2021.
38. Liu ZL, Liu ZJ, Liu JP, Yang M and Kwong J: Herbal medicines for viral myocarditis. Cochrane Database Syst Rev: CD003711, 2010.
39. Matsumori A, Wang H, Abelmann WH and Crumpacker CS: Treatment of viral myocarditis with ribavirin in an animal preparation. Circulation 71: 834-839, 1985.